

**REPORT DOCUMENTATION PAGE**

*Form Approved*  
OMB No. 0704-0188

The public reporting burden for this collection of information is estimated to average 1 hour per response, including the time for reviewing instructions, searching existing data sources, gathering and maintaining the data needed, and completing and reviewing the collection of information. Send comments regarding this burden estimate or any other aspect of this collection of information, including suggestions for reducing the burden, to Department of Defense, Washington Headquarters Services, Directorate for Information Operations and Reports (0704-0188), 1215 Jefferson Davis Highway, Suite 1204, Arlington, VA 22202-4302. Respondents should be aware that notwithstanding any other provision of law, no person shall be subject to any penalty for failing to comply with a collection of information if it does not display a currently valid OMB control number.

**PLEASE DO NOT RETURN YOUR FORM TO THE ABOVE ADDRESS.**

<b>1. REPORT DATE (DD-MM-YYYY)</b> 30-12-2009	<b>2. REPORT TYPE</b> Final Technical Report	<b>3. DATES COVERED (From - To)</b> 3/21/2006 - 9/30/2009
--	---	--

<b>4. TITLE AND SUBTITLE:</b> A Fluidic Dump Combustor for Ramjet Engines	<b>5a. CONTRACT NUMBER</b>
	<b>5b. GRANT NUMBER</b> N00014-06-1-0498
	<b>5c. PROGRAM ELEMENT NUMBER</b>

<b>6. AUTHOR(S)</b> Dr. David J. Forliti, Principal Investigator	<b>5d. PROJECT NUMBER</b> 09PR03229-01
	<b>5e. TASK NUMBER</b>
	<b>5f. WORK UNIT NUMBER</b>

<b>7. PERFORMING ORGANIZATION NAME(S) AND ADDRESS(ES)</b> The Research Foundation of SUNY Sponsored Projects Services 402 Crofts Hall Buffalo, NY 14260	<b>B. PERFORMING ORGANIZATION REPORT NUMBER</b> Project 1056402; Award 40073
---	---

<b>9. SPONSORING/MONITORING AGENCY NAME(S) AND ADDRESS(ES)</b> Office of Naval Research 495 Summer Street Suite 627 Boston, MA 02210-2109	<b>10. SPONSOR/MONITOR'S ACRONYM(S)</b> ONR
	<b>11. SPONSOR/MONITOR'S REPORT NUMBER(S)</b>

**12. DISTRIBUTION/AVAILABILITY STATEMENT**  
No restrictions.

**20100106191**

**13. SUPPLEMENTARY NOTES**

**14. ABSTRACT**  
Flame stabilization is the act of maintaining combustion in the presence of a high-speed premixed flow, and continues to be an important process that influences the performance and limitations for propulsion applications. A common approach for current generation flame holders involves the employment of a low-speed recirculation zone where hot combustion products are maintained and act as a continuous ignition source. The recirculation zone is often induced using a wake-generating bluff body that is submerged in the flow, or through the use of a rearward-facing step. A fluidic-based flame holder using a transverse slot jet issuing into a cross flow offers potential thrust and efficiency benefits for propulsion. The transverse slot jet flame holder has been shown to develop a low-speed recirculation zone capable of stabilizing a stationary flame, analogous to a rearward-facing step (i.e. a wall-bounded bluff body). The fluidic flame holder provides competitive flame holding performance to the mechanical counterpart, while having enhanced combustion rates that result in higher combustor efficiencies and/or shorter

**15. SUBJECT TERMS**

<b>16. SECURITY CLASSIFICATION OF:</b>			<b>17. LIMITATION OF ABSTRACT</b> UU	<b>18. NUMBER OF PAGES</b> 22	<b>19a. NAME OF RESPONSIBLE PERSON</b> Cynthia Pirson, Agreement Administrator
<b>a. REPORT</b> U	<b>b. ABSTRACT</b> U	<b>c. THIS PAGE</b> U			<b>19b. TELEPHONE NUMBER (Include area code)</b> 716-645-4407

# Final Report: A Fluidic Dump Combustor for Ramjet Engines

David J. Forliti  
*The State University of New York at Buffalo, Buffalo, NY 14221*

## Abstract

Flame stabilization is the act of maintaining combustion in the presence of a high-speed premixed flow, and continues to be an important process that influences the performance and limitations for propulsion applications. A common approach for current generation flame holders involves the employment of a low-speed recirculation zone where hot combustion products are maintained and act as a continuous ignition source. The recirculation zone is often induced using a wake-generating bluff body that is submerged in the flow, or through the use of a rearward-facing step. A fluidic-based flame holder using a transverse slot jet issuing into a cross flow offers potential thrust and efficiency benefits for propulsion. The transverse slot jet flame holder has been shown to develop a low-speed recirculation zone capable of stabilizing a stationary flame, analogous to a rearward-facing step (i.e. a wall-bounded bluff body). The fluidic flame holder provides competitive flame holding performance to the mechanical counterpart, while having enhanced combustion rates that result in higher combustor efficiencies and/or shorter burners. The mechanisms contributing to the enhanced combustion rates are discussed. Turbulent flame structures were investigated for various flame holders with emphasis on the downstream shear region. The role of baroclinic torque on turbulent flame structure evolution and the flowfield will be described. Comparisons will be made to a rearward-facing step flame holder. The details of the turbulent flow with combustion will be described, showing the potential advantages achieved using fluidics.

## I. Introduction

Turbulent combustion systems rely on flame holders in a premixed environment where inlet speeds are orders of magnitude larger than the laminar flame speed.<sup>1,2</sup> Flame holders provide two critical functions for these combustion systems. The primary function of the flame holder is to provide a flowfield environment where turbulent combustion is sustainable; this process is known as flame stabilization.<sup>1-12</sup> Flame stabilization is a complex combustion phenomenon involving both fluid dynamics and chemical kinetics to sustain a stabilized flame. The flame is stabilized through a sudden expansion where flow separation is introduced forming a low-speed recirculation zone acting as a continuous ignition source.<sup>1</sup>

The second important process assisted by the bluff body is the creation of turbulence that governs the transverse flame spread.<sup>13-16</sup> Turbulence produced in the reacting shear flow acts to wrinkle the flame, causing an increase in flame surface area and the reactant consumption rate. The increase in flame surface area results in a mean turbulent flame that travels at the turbulent flame speed with respect to the reactants. The turbulent flame speed may be significantly larger than the laminar flame speed. A high turbulent flame speed allows the mean flame to spread laterally into the high-speed reactant flow.

Bluff bodies are typical flame holders used in combustion systems.<sup>3</sup> The flame holder may be either a sudden expansion or a submerged bluff body, both types producing a recirculation region containing combustion products that act as an ignition source. The geometry of a flame holder varies depending on the application; however, bluff bodies are broadly characterized by their positions within the combustor: wall-bounded, and submerged.<sup>3</sup> Flame holder position influences flame stabilization performance and flame spread.<sup>15</sup> Similar to bluff bodies, fluidic flame holders are used to stabilize a flame.<sup>17</sup> The current research has shown that flame stabilization is achieved using a fluidic flame holder in the form of a transverse slot jet issuing into cross flow with a mechanism reminiscent of bluff bodies; however, the fluidic flame holder reduces thrust penalties associated with bluff-body drag by 5-15%.<sup>18</sup> Furthermore, lean/rich limits were dynamically controlled by the composition mixture and chemical nature of the jet fluid, allowing ultra-lean operating conditions. The research concluded that the size of the virtual fluidic flame holder is controlled dynamically by the jet blowing rate and scaled using the momentum ratio. The fluidic flame holder develops a downstream shear region due to the differential acceleration of reactants and products (governed by baroclinic torque) as shown in Fig. 1. This secondary shear region is formed at an earlier streamwise distance compared to an analogous bluff body configuration (a rearward-facing step), suggesting enhanced combustion-generated streamwise pressure gradients. The current paper describes the mechanisms responsible for the enhanced efficiency for the fluidic flame holder.

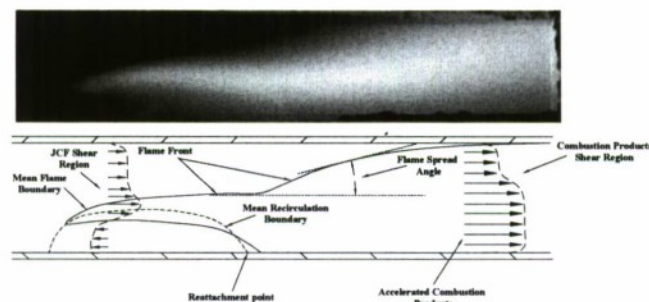


**Fig. 1 Chemiluminescence of mean flame and schematic of the fluidic flame holder flow features**

## II. Experimental Setup

The experiments were conducted in the Combustion Laboratory in the Mechanical and Aerospace Engineering Department at The State University of New York at Buffalo. Figure 2 shows the schematic of the fluidic dump combustor. Regulated and metered main air flow is supplied to the plenum of the ramjet model facility. The plenum of the test rig contains flow conditioning which is described in detail by Ahmed and Forliti.<sup>18</sup> A section of the manifold for the slot jet is shown in the figure. The flow path of the slot jet has two sudden contractions in series and multiple screens were added to establish spanwise uniformity. The slot jet has a short dimension of 0.279 mm and is expected to be fully-developed.<sup>18</sup>

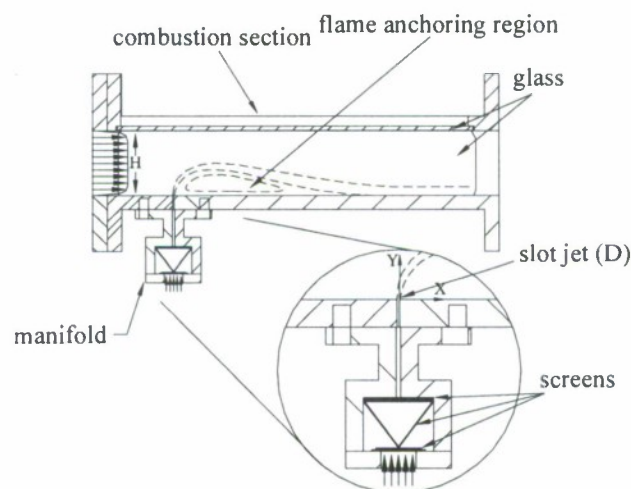
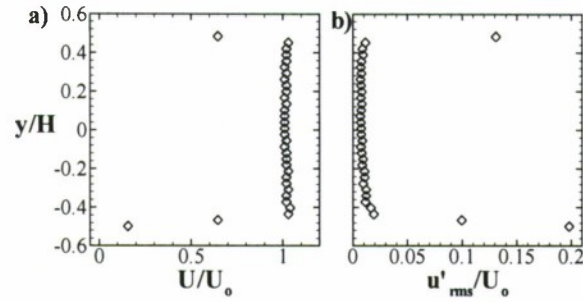


Fig. 2 Schematic of the fluidic flame holder flow features

The velocity  $U_0$  used for scaling is the mean velocity at the combustor inlet and is nominally 11 m/s. The Reynolds number based on combustor height was held constant at approximately 32000. The initial conditions of the combustor were altered to provide a top-hat velocity profile compared to the quasi-parabolic profile of the previous investigation by Ahmed and Forliti.<sup>18</sup> Figure 3 shows profiles of the mean and rms fluctuation of the streamwise velocity at the inlet of the combustor. The channel flow and the fluidic stream were set to have an equivalence ratio of  $\phi = 1$  under reacting conditions using methane (99% pure) as fuel. The combustion section height  $H$  was used to normalize dimensional scales; the cross section is 45 mm x 127 mm.



**Fig. 3 Profiles of (a) mean streamwise velocity and (b) rms of streamwise velocity fluctuation at the combustor inlet**

Digital particle image velocimetry (DPIV) was used to study the velocity field of the transverse slot jet under nonreacting and reacting conditions. An IDT system was used for DPIV employing ProVISION-XS software and an X-stream VISION camera. A New Wave Research Solo PIV III Nd:YAG laser capable of 50 mJ/pulse (532 nm) at 15 Hz is used as a light source. Images were processed using 64 x 32 pixel interrogation regions with 50% overlap, resulting in a spatial resolution of 3.136 mm in the streamwise direction and 1.568 mm in the cross stream direction. Aluminum oxide particles of 0.5 micron diameter were used for seeding. Generally 800 image pairs were collected for each case. Uncertainties due to precision error were found to be 0.015 pixels for 95% confidence. The bias error could be approximated according to Forliti et al. and was addressed by Ahmed et al.<sup>19, 20</sup> The mean and rms fluctuation velocities were known to within approximately 3 and 4% of the channel flow maximum velocity  $U_0$ , respectively.

### III. Results and discussion

The current research investigating fluidic and bluff-body flame holders has identified turbulent flame structures that influence flame spread and combustion rate. Although the flame stabilization mechanism principle is similar for both flame holders, the difference in the evolution of the flame topology had an apparent effect on the combustion rate. The evolution of the turbulent structure for the confined stabilized premixed flames is unique as the flowfield evolution including a reversal in mean shear as shown in Fig 1. Structures that form in the near field of the recirculation zone will tend to have clockwise rotation. These structures convect and enter the downstream region where they experience a mean flow that will tend to reverse the rotation direction.

Unsteady flow structures have been a focus of interest for decades for reacting and nonreacting shear flows.<sup>21, 22</sup> Brown and Roshko found that vortex-like structures were formed in a mixing shear layer; studying these structures

has provided fundamental insight into the physical processes that influence spatial development of shear layers.<sup>21, 22</sup> Exercising the same principle of analyzing the flame structures of both flame holders will further explain the mechanisms through which fluidic injection enhances combustion.

Flame spread is the process by which the combustion front propagates transversely across the flow path and governs the required combustor length to achieve high combustion efficiency. Flame spread was investigated under the current research, identifying key flame structures that govern the transverse transport of the flame in the downstream secondary shear region.<sup>23</sup> Random instantaneous PIV images of the reacting flow were extracted to represent the turbulent flame structures under reacting conditions ( $\Phi = 1$ ). The stark density difference in seed particles caused by the volumetric expansion allows for the visualization of the flame region. Four images were used to construct a full combustor length image at each consecutive streamwise location. The images were chosen to approximately match the turbulent structures present in the flow from the previous image in the streamwise distance; the images were taken with one camera, hence they are not simultaneous images. Four constructed instantaneous PIV images were randomly chosen for each flame holder. The instantaneous PIV images provide qualitative measures of the flame geometry present in the reacting flowfield. Figure 4 shows the spatial distribution of the wrinkled flame structure for both a backward-facing step and fluidic flame holder. The evolution of the turbulent flame wrinkles is governed by flame propagation and the local unsteady shear flow. The flame structures' characteristics varied between the various flame holders. In the bluff-body flame holder cases shown in Fig. 4(a-d), the structures induce transport of reactants downward into the products region with relatively weak upward propagation of the bulk flame. This entrainment mechanism results in production of flame surface area mainly in the lower half of the combustor. The bluff body configuration tends to indicate that the downstream structures appear to be evolved versions of the clockwise rotating structures formed near the bluff body, whereas the fluidic case shows much more chaotic flame topology. For the fluidic flame holder, the turbulent structures form at the location of initial instability between the jet and main flow interaction and evolve downstream allowing combustion products to propagate into and consume reactants near the top wall, as shown in Fig. 4(d-g). These structures appear to enhance the fluidic flame holder efficiency and flame spread compared to the bluff-body flame. It is hypothesized that the enhanced turbulent transport caused by the jet is responsible for the observed difference in the flame structure.

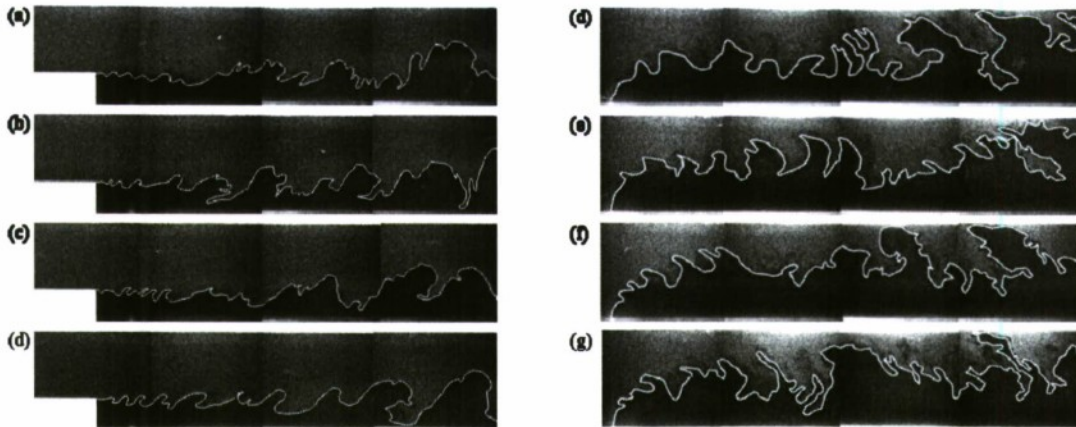


**Fig. 4 Instantaneous PIV images of the flame structure for the (a-d) step flame holder and (d-g) fluidic flame holder**

Figure 5 shows a schematic explaining the theory of turbulent flame structure development for each flame holder. The structures for the bluff body initially form a clockwise rotation due to the negative vorticity produced by the no-slip boundary condition on the top surface of the bluff body. The negative vorticity entrains reactants into the product region where they are consumed. Due to flame propagation, the flame sheet will separate from the vorticity-laden region and propagate into the main flow. The transverse jet introduces highly turbulent fluid with both positive and negative vorticity, resulting in intensified flame wrinkling. Pockets of intense combustion are able to propagate upwards with an enhanced turbulent flame speed and approach the top wall of the combustor as shown in Fig 4. It is interesting to note that these pockets that are able to propagate to the upper wall are intermittent.

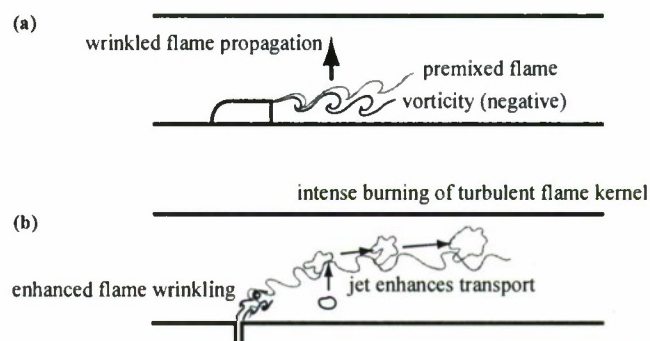


**Fig. 5 Schematic of the mechanisms influencing the evolution of the turbulent flame structures for (a) bluff-body flame holder, and (b) fluidic flame holder**

The initial flame wrinkling process is governed by the characteristics of the vorticity field near the leading edge of the flame holder. For the rearward-facing step, the vorticity that is shed at the trailing edge is negative due to the boundary layer, confirming the observation in Fig. 4 that the structures initially have a clockwise rotation. However, when investigating the mean vorticity field a positive vorticity is observed in the downstream region, as shown in

Fig. 6(b). This suggests that although the structures initially formed have a clockwise rotation due to negative vorticity present, as the structures grow in time and space, other mechanisms are present downstream that influence the orientation of the structures. The fluidic flame holder forms positive and negative vorticity initially due to the jet boundary condition, as shown in Fig. 6(d). This positive vorticity is further enhanced due to the baroclinic torque formed along the flame interface, whereas, the negative vorticity is concentrated within the recirculation zone. The flame-generated vorticity for the fluidic flame holder evolves downstream, transporting combustion products into the reactant stream allowing the flame to consume reactants at a high turbulent flame speed. The bluff-body however, produces positive vorticity downstream that is present within the combustion products region counteracting the flame structures formed initially from the negative vorticity of the boundary condition; a region of weak mean vorticity is present for  $x/H$  between 2 and 3 for the bluff body.

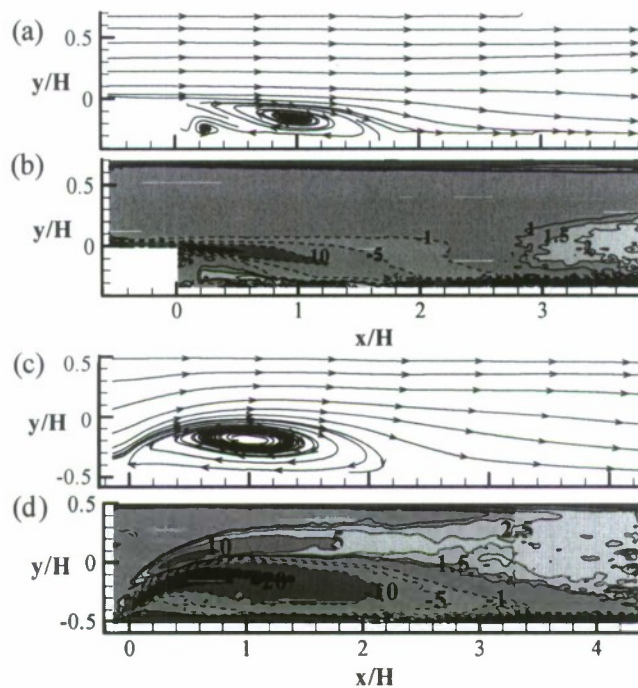
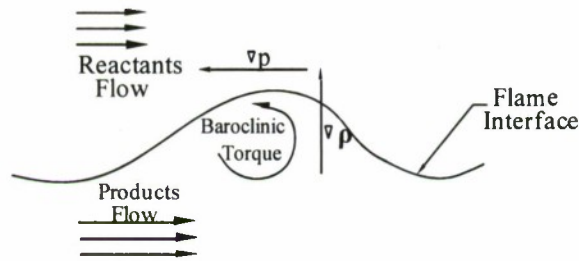


**Fig. 6 Mean bluff-body flame (a) streamlines, (b) vorticity field, and mean fluidic flame holder (c) streamlines, (d) vorticity**

The Baroclinic torque is one of the main mechanisms contributing to the evolution of the flame structures.<sup>24-33</sup> The misalignment of the streamwise pressure gradient along the length of the combustor and the cross-stream density gradient associated with a locally non-vertical flame element produces vorticity within the flame through the baroclinic torque mechanism. Figure 7 shows a schematic of the baroclinic torque generation mechanism at the

flame interface in the presence of an orthogonal pressure and density gradients. The resulting vorticity created can either suppress or amplify the flame wrinkles, influencing the flame sheet evolution. As shown in the vorticity transport equation (Eq. 1), the only source of vorticity generation is the baroclinic torque term.<sup>26</sup> The second term on the right hand side of Eq.1 represents volume expansion term which is not a source of vorticity. The vorticity stretching term stretches existing vorticity, also not a source of new vorticity. The diffusion term causes a spreading of the vorticity in space and a reduction of the local vorticity but does not change the total vorticity (i.e. the circulation).<sup>26</sup> Previous studies have employed the vorticity transport equation in computational fluid dynamics to better understand the role of baroclinic torque on the flame front of bluff bodies.<sup>27, 28, 30, 31</sup> Experimental studies of the baroclinic torque was limited to focusing on laminar unconfined flames.<sup>26, 29, 32, 33</sup> These studies have shown that although flame wrinkling is influenced by the flame surface area, geometry, and burning velocity variation, the baroclinic torque consequently contributes to the flame wrinkling. This is established through affecting the flowfield of the combustion products leading to flow patterns that influence the flame wrinkling.<sup>32</sup> The increase in flame wrinkling will increase the flame surface area leading to higher reactants consumption and enhanced efficiency. This mechanism is known to produce flame-generated vorticity which counteracts the reduced amplitude of flame wrinkling caused by the gas expansion.<sup>34</sup>

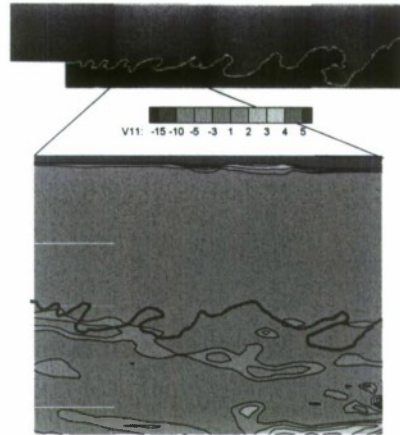
$$\frac{D\bar{\omega}}{Dt} = \underbrace{\frac{1}{\rho^2}(\bar{\nabla}\rho \times \bar{\nabla}p)}_{\text{Baroclinic Torque}} - \underbrace{\bar{\omega}\bar{\nabla}\cdot\bar{v}}_{\text{Gas Expansion}} + \underbrace{\bar{\omega}\cdot\bar{\nabla}\bar{v}}_{\text{Vorticity Stretching}} + \underbrace{\nu\nabla^2\bar{\omega}}_{\text{Vorticity Diffusion}} \quad (1)$$



**Fig. 7 schematic of the baroclinic torque generation mechanism at the flame interface**

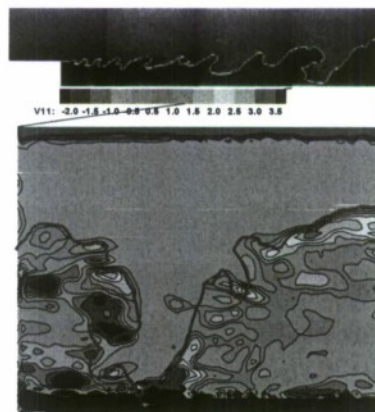
Figure 8 shows the upstream flame structures and instantaneous vorticity for a bluff-body flame. Examining the upstream instantaneous vorticity field, negative vorticity is formed by the bluff-body boundary condition. This negative vorticity influences the shape and rotation of the structures. Separation between the flame interface and the negative vorticity is due to flame propagation. Weak positive vorticity generation is present near the bottom wall

due to the viscous shear between the reverse velocity of the recirculation zone and the bottom combustor wall (the boundary layer is not adequately resolved).



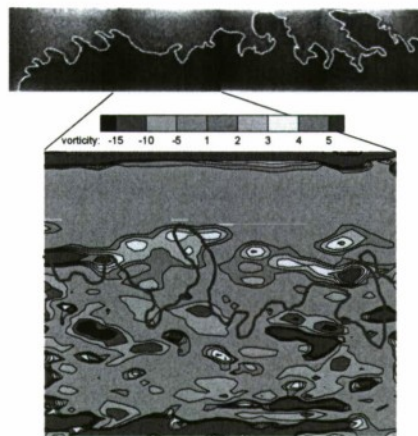
**Fig. 8 Upstream flame structures and instantaneous vorticity for bluff-body flame**

Downstream, the instantaneous vorticity is concentrated at the flame interface, as shown in Fig 9. A clear positive vorticity is noticed at the flame boundaries, it is thought to be due to baroclinic torque within the flame. Areas of negative vorticity are present in the field; however, the positive vorticity formed by the baroclinic torque will cancel the negative vorticity as the structures evolve. It is also possible for negative vorticity to be generated via the baroclinic mechanism due to unsteady pressure gradients and/or local negative vertical density gradients due to a highly convoluted flame surface. The positive vorticity is expected to change the rotation of the flame structures at a much further distance downstream to a counter clockwise rotation. Since the fluidic flame holder contains positive vorticity throughout, the baroclinic torque is more likely to assist in producing velocity fluctuations that will enhance flame wrinkling processes.



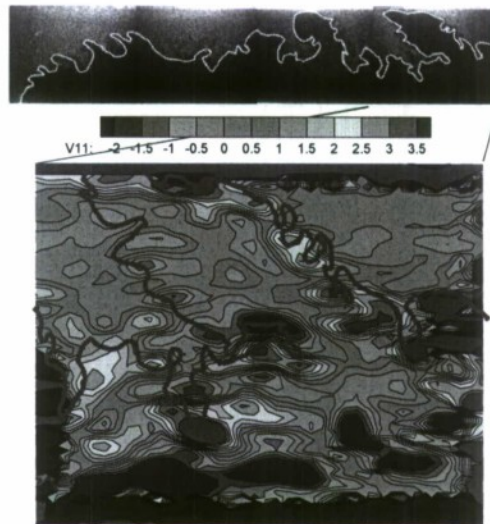
**Fig. 9 Downstream flame structures and instantaneous vorticity for the bluff-body flame**

For the fluidic flame holder, the vorticity of the transverse jet also contributes to the evolution of the turbulent flame structures. Compared to the instantaneous vorticity of the bluff body, the fluidic flame holder produces a convoluted vorticity field with positive and negative vorticity in the flame stabilization region, as shown in Fig. 10. High levels of vorticity, with magnitudes that are governed by the jet and not the main flow, cause intense flame wrinkling in the near field. The negative vorticity is submerged within the recirculation zone, and the positive vorticity is present at the flame interface. The positive vorticity is associated counter-clockwise structures that transport combustion products upwards into the high-speed main flow.



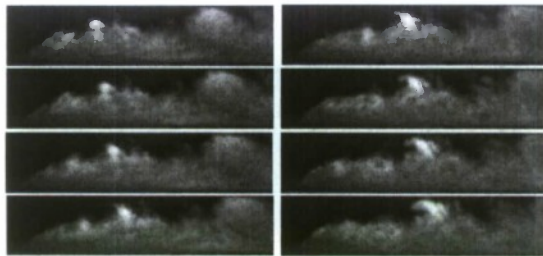
**Fig. 10 Upstream flame structures and instantaneous vorticity for fluidic flame holder**

Figure 11 shows the details of the flame and vorticity in the downstream region of the fluidic flame holder. The large region of products is believed to be caused by flame propagation after the initial transport of hot turbulent gases by the transverse jet. The influence of baroclinic torque is evident on the upstream and downstream flame boundary of the large structure. The left flame boundary of the structure forms negative vorticity at the interface due to the downward component of the density gradient at the flame and the pressure gradient oriented upstream. The right flame boundary of the structure produces positive vorticity at the interface due to the upward density gradient increasing along the streamwise direction. The flame along these boundaries is seen to be highly convoluted and indicate rotation consistent with the nearby flame-generated vorticity. This further confirms the important role of the baroclinic torque on enhancing the combustion process.



**Fig. 11 Downstream structures and instantaneous vorticity for fluidic flame holder**

Chemiluminescence measurements were collected using a high-speed intensified camera, to better understand the mechanisms that influence the evolution of the turbulent flame structures for the fluidic flame holder. Figure 12 shows a sequence of chemiluminescence images of the turbulent flame structures for the fluidic flame holder. The intensity is approximately proportional to the burning heat release rate. A turbulent heat release structure is clearly identified forming from the jet interaction with the main flow and amplifies as it convects downstream. The intense combustion near the outer edge of the flame stabilization region is able to rapidly propagate across the combustor to the top wall. The heat release structures correlates with the turbulent flame structure observed in Fig. 4. It is apparent that the formation of moderate to high intensity burning structures that can penetrate across the channel is quasi-periodic. This phenomenon appeared to be periodic with a frequency of  $200 \pm 10$  Hz. It is suggested that this is not a thermo-acoustic oscillation as the main flow does not contain velocity fluctuations that are typical of resonating combustors.



**Fig. 12 Sequence of instantaneous chemiluminescence images of the fluidic flame holder**

Further downstream, the fluidic flame holder has shown to produce flame structures with counter-clockwise rotation. The baroclinic torque influences the flame structures' rotation and is the only source of flame-generated vorticity. Figure 13(c) shows the mean pressure measured along the upper wall with and without combustion, along with an instantaneous flame visualization (Fig. 13(a)) and the mean streamwise velocity (Fig. 13(b)) that shows the two shear flow regions. The pressure gradients in the upstream half of the flame stabilization region are caused by the flow acceleration due to the blockage of the main flow by the transverse jet.

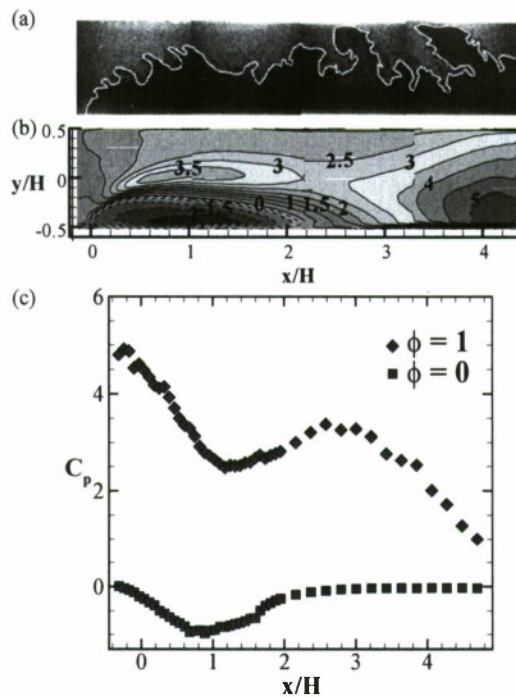


**Fig. 13 Fluidic flame holder (a) instantaneous PIV image, (b) mean velocity field, (c) mean pressure at the top wall**

To further quantify the vorticity present in the flow field of both flame holders, probability distribution functions (PDF) of the vorticity were constructed. Figure 14 shows the vorticity PDF for both flame holders in the flame stabilization region. The PDF of vorticity for the bluff body shows presence of predominantly negative vorticity whereas the fluidic flame holder shows a distribution of positive and negative vorticity which is due to the vorticity of the jet. Although the fluidic flame holder shows a high peak of negative vorticity compared to the positive vorticity, the percentage of positive vorticity is higher. It should be noted that the PIV data cannot resolve the small scales of the jet, hence the vorticity is spatially filtered.

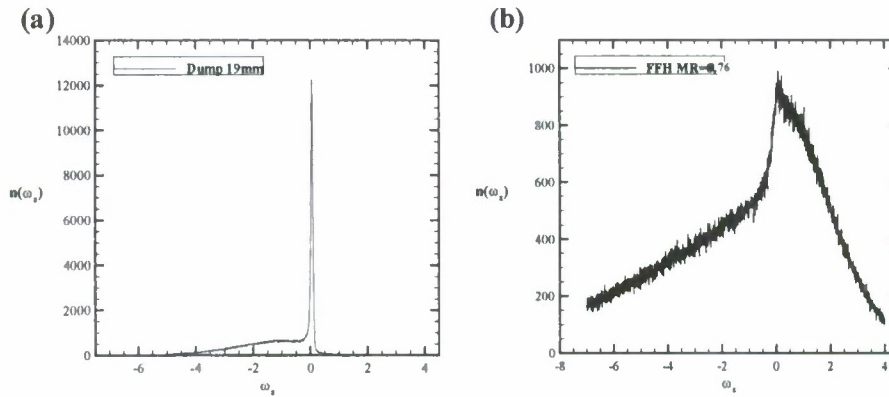


**Fig. 14 PDF of vorticity in the flame stabilization region for the (a) bluff-body flame holder and (b) Fluidic flame holder**

Figure 15 shows the downstream vorticity PDF for both flame holders. The vorticity PDF of the bluff body shows a centered distribution, when compared to the upstream PDF it is noticeable that positive vorticity is produced in the downstream and negative vorticity is reduced. The fluidic flame holder shows an asymmetric distribution of vorticity showing higher positive vorticity production.

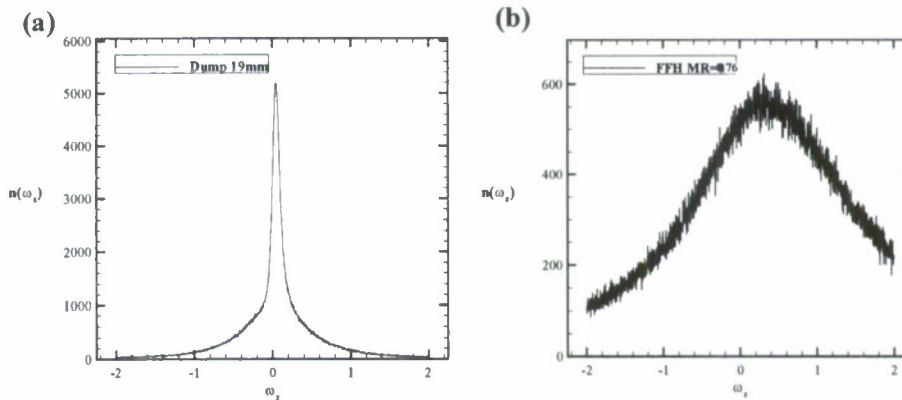


**Fig. 15 Downstream Vorticity PDF for the (a) bluff-body flame holder, (b) Fluidic flame holder**

High-resolution PIV data was collected to better resolve the vorticity present along the jet trajectory. Figure 16 shows the mean vorticity field for the fluidic flame holder under nonreacting and reacting conditions. It is clear that the vorticity increased under reacting condition which is due to the presence of baroclinic torque. It is interesting to note that the mean vorticity was enhanced for both the negative and positive regions of the jet. It is expected that the positive vorticity would be enhanced due to the pressure field shown in Fig. 13(c). The enhanced vorticity and apparent circulation in the negative region of the jet is unexpected. It is unlikely that the initial vorticity of the jet is

changed due to combustion due to the high jet velocity (i.e. the dynamic pressure of the transverse jet is much larger than the dynamic pressure of the main flow). The pressure field away from the boundaries is unavailable and may be responsible for establishing baroclinic torque that enhances the negative vorticity.

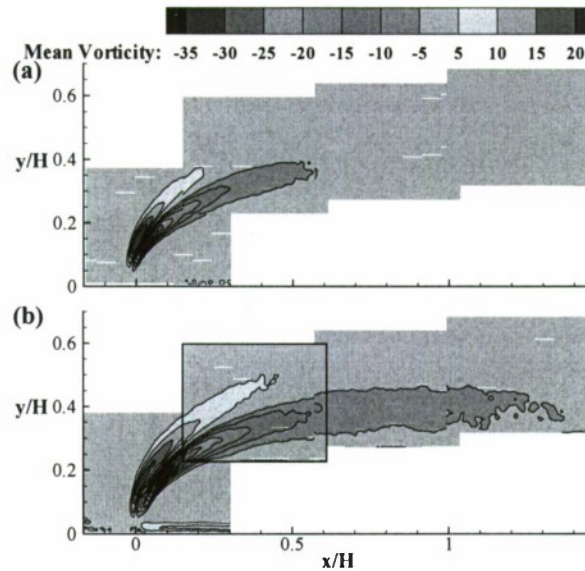


**Fig. 16 High resolution mean vorticity along the mean flame interface under (a) nonreacting and (b) reacting conditions**

Beyond the baroclinic torque and positive vorticity present upstream, the jet turbulence is another mechanism that contributes to the process of entraining combustion products in the reactants field. It was thought that by increasing the turbulence intensity of the velocity fluctuations, a larger volume of reactants would be consumed due to the increased flame wrinkling; however, the magnitude of the vertical velocity fluctuations is also expected to influence the evolution of flame structures through enhancing the transport of combustion products across transverse jet shear flow region. Once the combustion products surpass the velocity gradients of the jet in cross flow shear and into the reactants, it is then free to consume reactants while traveling along the combustor with the local reactants velocity and is no longer inhibited by high strain-rate regions in the reactants.

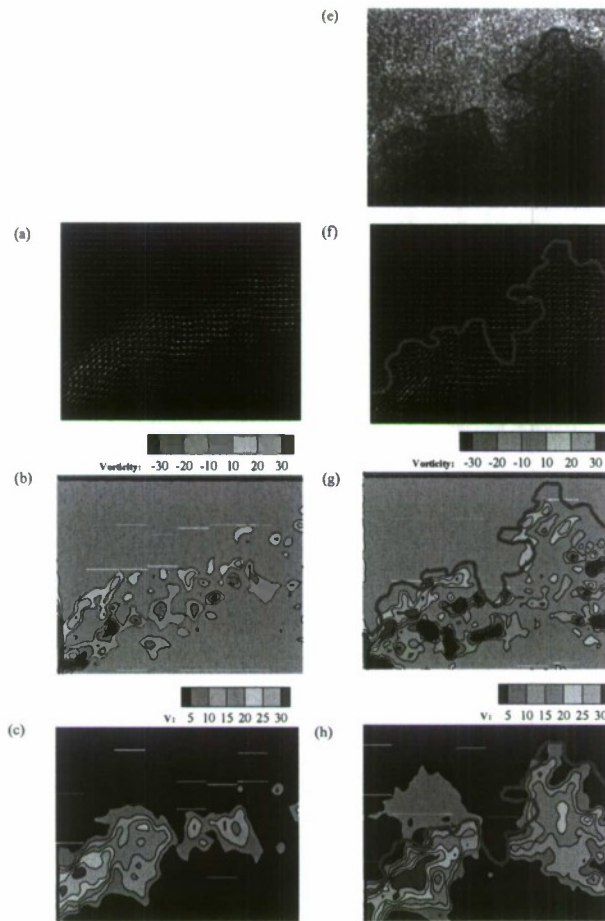
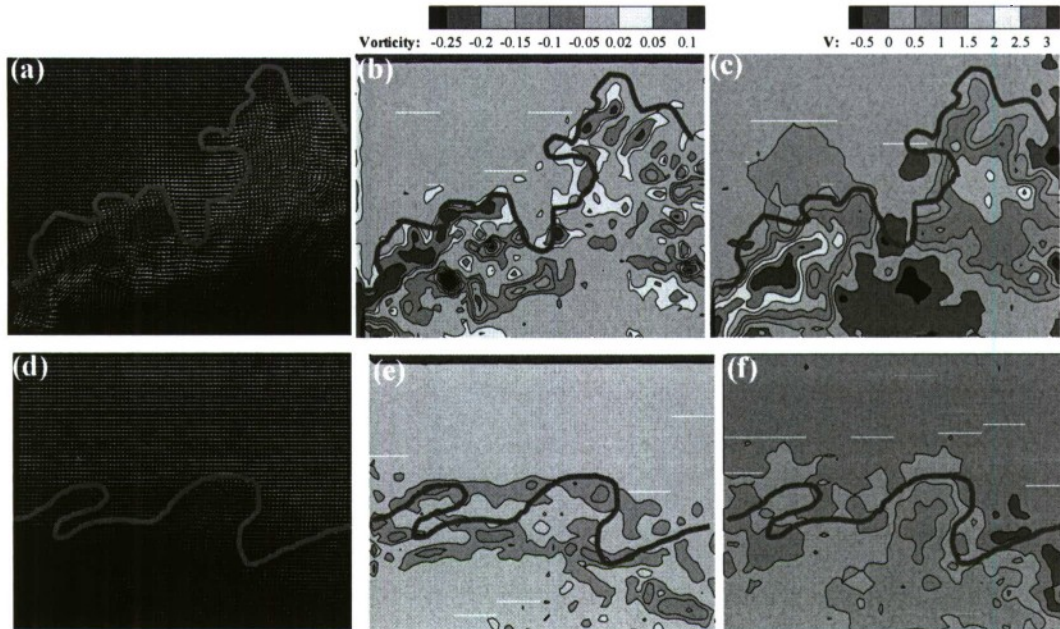


**Fig. 17 Instantaneous nonreacting (a) vector field, (b) vorticity, (c) vertical velocity and reacting (d) PIV image, (e) vector field, (f) vorticity, (g) vertical velocity**

Figure 17 shows the instantaneous velocity-vector field, vorticity, vertical velocity and PIV image for nonreacting and reacting conditions, located  $0.2H$  downstream of the jet as framed in Fig. 16. The positive vorticity increased under reacting conditions due to the baroclinic torque discussed earlier; however, the instantaneous vertical velocity shows an increase at locations along the flame interface where structures appear to form. The vertical velocity peaks at  $2.7U_0$  which is a relatively high velocity compared to the main stream velocity. The high vertical velocity results in the penetration of combustion products upwards into the main reactant flow.

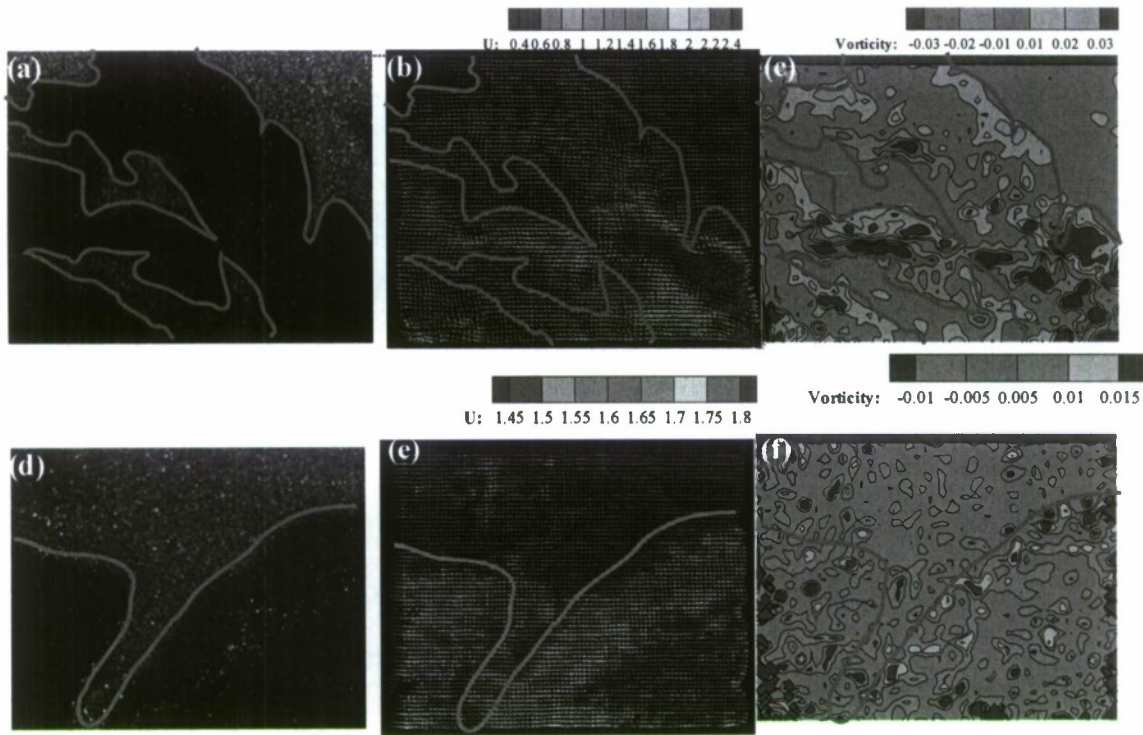
Figure 18 shows instantaneous vector field, vorticity, vertical velocity for fluidic flame holder and bluff-body flame holder. When compared to the bluff body, the fluidic flame holder produces positive vorticity along the flame surface due to baroclinic torque. Since the PIV frame shown is at an early streamwise distance,  $x/H = 0.2$ , the negative vorticity produced by the bluff body coincides with the flame surface. The vertical velocity is shown to be

present at the location of the structure formation for the bluff body peaking at a velocity approximately equal to the main flow velocity; however, the fluidic flame holder shows a much higher vertical velocity peaking at three times the main flow velocity. This further confirms the enhanced transport produced by the get turbulence. The coupling of both mechanisms, the vertical velocity fluctuations and the vorticity influence the turbulent flame structures formation and evolution.



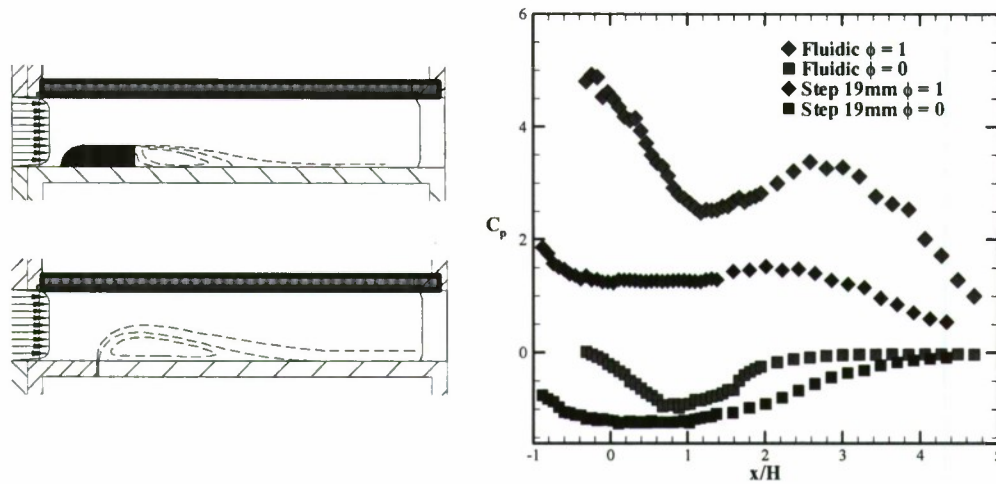
**Fig. 18 Upstream instantaneous fluidic flame holder (a) vector field, (b) vorticity, (c) vertical velocity and bluff-body flame holder (d) vector field, (e) vorticity, and (f) vertical velocity**

Figure 19 shows instantaneous PIV image, velocity-vector field, and vorticity for the fluidic and bluff-body flame holders in the downstream region centered at  $x/H = 3.5$ . The fluidic case shows a structure developed downstream. Positive and negative vorticity produced due to baroclinic torque is present at the flame surface. Vorticity will continue to form at the flame surface due to the mean pressure gradient unless the local flame element is vertical. The bluff body shows the clockwise structures in that frame. Vorticity generation is shown along the flame surface.



**Fig. 19 Downstream instantaneous fluidic flame holder (a)PIV images, (b) vector field, (c) vorticity and bluff-body flame holder (d) PIV images, (e) vector field, and (f) vorticity**

The mean vorticity for the fluidic flame holder has shown an increase in positive and negative vorticity at the jet location from nonreacting conditions to reacting conditions. This increase is observed in Fig. 16. It was believed that the increase in positive vorticity is due to baroclinic torque present along the jet trajectory. This is further confirmed when mean pressure measurements were collected along the top surface of the combustor. The nondimensional mean pressure measurements at the top wall are shown in Fig. 20. The pressure at the top wall is initially high at the injection location ( $x/H = 0$ ) where the jet partially blocks the main flow and gradually decreases along the streamwise distance forming a pressure gradient pointing upstream. The upstream pointing pressure gradient coupled with the density pointing towards the top wall forms a baroclinic torque which further increases/enhances the positive vorticity produced by the jet under reacting conditions along the top trajectory of the jet.



**Fig. 20 Mean pressure distribution at the top wall for the fluidic and bluff-body flame holder**

Negative vorticity has shown to also increase under reacting conditions which contradicted the role of baroclinic torque producing positive vorticity. However, when mean pressure measurements were collected along the bottom surface of the combustor, it was found that a pressure gradient is pointing downstream. The pressure gradient pointing downstream along with density gradient pointing to the top wall forms a baroclinic torque which further increases/enhances the negative vorticity produced by the jet under reacting conditions along the bottom trajectory of the jet. The nondimensional mean pressure measurements at the bottom wall are shown in Fig. 21. The pressure at the bottom wall is initially low at the injection location ( $x/H = 0$ ) where the high velocity jet causes high entrainment producing a low pressure region and gradually increases along the streamwise distance as the pressure is recovered forming a pressure gradient pointing downstream.

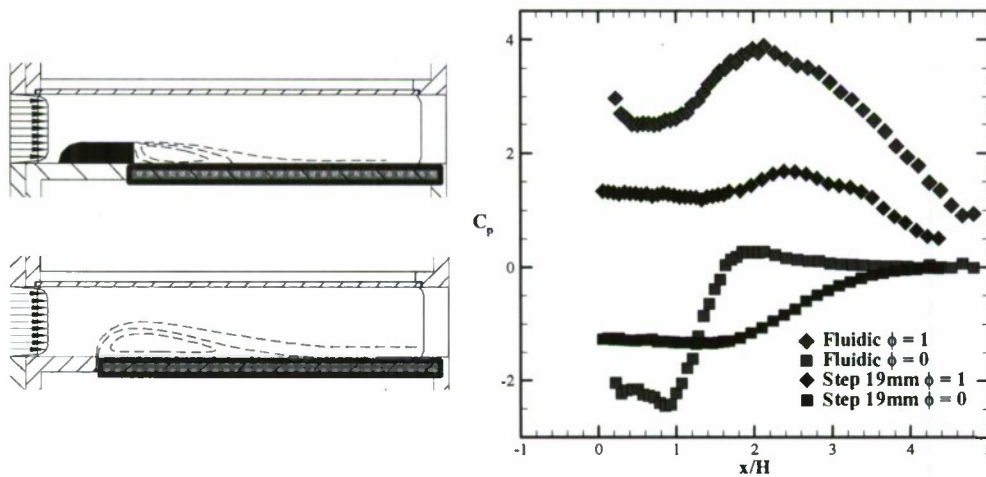


**Fig. 21 Mean pressure distribution at the bottom wall for the fluidic and bluff-body flame holder**

Heat release spectra measurements were documented in order to identify combustion instabilities. The spectra were calculated from a time-resolved measure of the light emission captured from the flame stabilization region. Figure 22 shows the heat release spectra for both flame holders. There is a peak frequency that is present for both flame holders. The peak frequency for the fluidic flame holder is believed not to be due to thermo-acoustic instability, since the velocity fluctuations upstream of the jet measured using PIV are weak; the transverse jet would also interfere with receptivity to background acoustic perturbations. It is hypothesized that the instabilities present maybe due to global instabilities caused by the fluid dynamics of the jet.

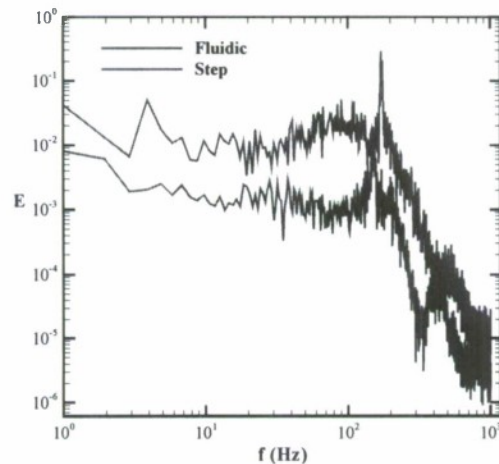


**Fig. 22 Heat release spectra for both fluidic and bluff-body flame holder**

Figure 23 shows the scaling of the peak frequency using two different Strouhal number definitions at different momentum ratios. It is interesting to note that when scaled using the maximum streamwise velocity at the middle of the recirculation zone, the range of Strouhal numbers was in agreement with that proposed by Ghoniem et al. for combustion oscillations driven by hydrodynamic global instabilities.<sup>35</sup> Current research is begin conducted on linear stability analysis of the experimental profiles to determine if the flow is locally absolutely unstable, a precondition for global instability.

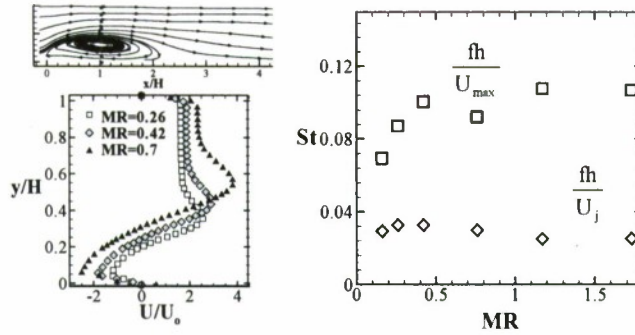


Fig. 23 Peak frequency scaling using the Strouhal number at different momentum ratios

The ratio of minimum to maximum velocity at half recirculation length also appears to scale with the momentum ratio, as shown in Fig. 24. This further suggests that global instability maybe be present.<sup>36-38</sup>

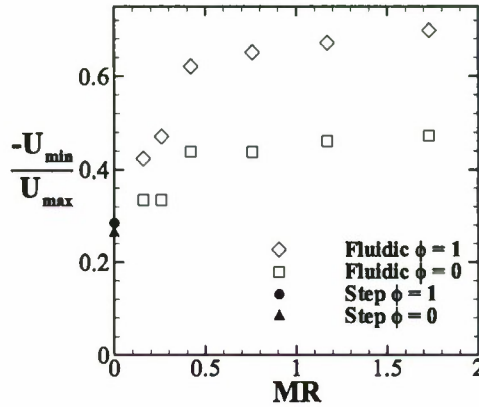


Fig. 24 Scaling of minimum to maximum velocity ratio with momentum ratio

#### IV. Conclusion

The current research explored the Mechanisms influencing the evolution of turbulent flame structure for a fluidic flame holder using a confined transverse slot jet in a channel flow. The fluidic flame holder had counter clockwise rotating flame structures that allowed flame spread to the top wall compared to a bluff-body flame holder where the flame structures had clockwise rotation limiting combustion products from propagation in the reactants. Flame-generated vorticity was shown to enhance flame spread in the downstream region enhancing efficiency of the combustor. Baroclinic torque was shown to produce positive vorticity in the downstream. Instantaneous vorticity fields were explored for both bluff-body and fluidic flame holder showing higher positive vorticity produced by the fluidic flame holder which enhances transport of combustion products in to reactants. Flame structures appearing from the jet trajectory and evolving downstream in to large structures were explored for the fluidic flame holder.

The mechanisms influencing these structures were isolated to baroclinic torque enhancing the positive vorticity produced by the jet boundary, and the turbulent vertical velocity of the jet enhancing the transport of combustion products in to reactants. The positive and negative vorticity was shown to increase under reacting conditions at the initial jet interaction with the cross flow. The increase in vorticity was due to the presence of baroclinic torque. The turbulent vertical velocity of the jet contributed to transporting combustion products in to reactants past the high shear region, allowing local flame propagation and a very different structure to the flame. The instantaneous vertical velocity fields have shown the formation of the structures where the vertical velocity was peaking an order of magnitude higher than the main flow velocity. Fluidic flame structure continues to enhance in the secondary shear region. These flame structures that form in the fluidic flame holder case enhance efficiency of the combustor compared to a bluff-body flame holder.

## References

- <sup>1</sup>Longwell, J.P., Frost, E.E., and Weiss, M.A., "Flame Stability in Bluff Body Recirculation Zones," *Industrial & Engineering Chemistry*, Vol. 45, No. 8, 1953, pp. 1629-1633.
- <sup>2</sup>Williams, G., Hottel, H., and Scurlock, A., "Flame Stabilization and Propagation in High Velocity Gas Streams," *Proceedings of the Combustion Institute*, Vol. 3, 1951, pp. 21-40.
- <sup>3</sup>Longwell, J.P., "Flame Stabilization by Bluff Bodies and Turbulent Flames in Ducts," *Proceedings of the Combustion Institute*, Vol. 4, 1953, pp. 90-97.
- <sup>4</sup>Ozawa, R.I., "Survey of Basic Data on Flame Stabilization and Propagation for High Speed Combustion Systems", in *AFAPL-TR-70-81*. 1971, The Marquart Co.
- <sup>5</sup>Rizk, N.K. and Lefebvre, A.H., "Influence of Laminar Flame Speed on the Blowoff Velocity of Bluff-Body-Stabilized Flames," *AIAA Journal*, Vol. 22, No. 10, 1984, pp. 1444-1447.
- <sup>6</sup>Thurston, D., "An Experimental Investigation of Flame Spreading from Bluff Body Flameholders," *Aeronautical Engineering*, California Institute of Technology, Pasadena, CA, 1958.
- <sup>7</sup>Pitz, R.W. and Daily, J.W., "Combustion in a Turbulent Mixing Layer Formed at a Rearward-Facing Step," *AIAA Journal*, Vol. 21, No. 11, 1983, pp. 1565-1570.
- <sup>8</sup>Armaly, B.F., Durst, F., Pereira, J.C.F., and Schoenung, B., "Experimental and Theoretical Investigation of Backward-Facing Step Flow," *Journal of Fluid Mechanics*, Vol. 127, 1983, pp. 473-496.
- <sup>9</sup>Penner, S.S. and Williams, F., "Recent Studies on Flame Stabilization of Premixed Turbulent Gases," *Applied Mechanics Reviews*, Vol. 10, No. 6, 1957, pp. 229-237.
- <sup>10</sup>Bush, S.M. and Gutmark, E.J., "Reacting and Non-Reacting Flow Fields of a V-Gutter Stabilized Flame", in *44th AIAA Aerospace Sciences Meeting and Exhibit*. 2006. pp. 1-11.
- <sup>11</sup>Williams, G.C., Woo, P.T., and Shipman, C.W., "Boundary Layer Effects on Stability Characteristics of Bluff Body Flameholders," *Proceedings of the Combustion Institute*, Vol. 6, 1957, pp. 427-438.
- <sup>12</sup>Erickson, R.R., Soteriou, M.C., and Mehta, P.G. "The Influence of Temperature Ratio on the Dynamics of Bluff Body Stabilized Flames" *AIAA Aerospace Sciences Meeting and Exhibit*, Reno, NV, 2006, pp. 1-18.
- <sup>13</sup>Wright, F.H. and Zukoski, E.E., "Flame Spreading from Bluff-Body Flame Holders," *Proceedings of the Combustion Institute*, Vol. 8, 1962, pp. 33-43.
- <sup>14</sup>Spalding, D.B., "Theory of Rate of Spread of Confined Turbulent Premixed Flames," *Proceedings of the Combustion Institute*, Vol. 7, 1959, pp. 595-603.
- <sup>15</sup>Williams, F. "Flame Stabilization of Premixed Turbulent Gases", *Applied Mechanics Surveys*, 1966, pp. 1157-1170.
- <sup>16</sup>Bjerklie, J.W. "Aerothermochemical Aspects of Flame Holder Performance", *Proceedings of Gas Dynamics Symposium*, North-western University, 1955, pp. 221-232.
- <sup>17</sup>Schaffer, A. and Cambel, A.B., "The Effect of Opposing Jet on Flame Stability," *Jet Propulsion*, Vol. 25, 1955, pp. 284-287.
- <sup>18</sup>Ahmed, K.A. and Forliti, D.J., "Fluidic Flame Stabilization in a Planar Combustor Using a Transverse Slot Jet," *AIAA Journal*, Vol. 47, No. 11, 2009, pp. 2770-2775.

- <sup>19</sup>Forliti, D.J., Strykowski, P.J., and Debatin, K., "Bias and Precision Errors of Digital Particle Image Velocimetry," *Experiments in Fluids*, Vol. 28, No. 5, 2000, pp. 436-447.
- <sup>20</sup>Ahmed, K.A., Forliti, D.J., Moody, J.K., and R., Y., "Flowfield Characteristics of a Confined Transverse Slot Jet," *AIAA journal*, Vol. 46, No. 1, 2008, pp. 94-103.
- <sup>21</sup>Clavin, P. and Williams, F.A., "Effects of Molecular Diffusion and of Thermal Expansion on the Structure and Dynamics of Premixed Flames in Turbulent Flows of Large Scale and Low Intensity," *Journal of Fluid Mechanics*, Vol. 116, 1982, pp. 251-282.
- <sup>22</sup>Brown, G.L. and Roshko, A., "On Density Effects and Large Structure in Turbulent Mixing Layers," *Journal of Fluid Mechanics*, Vol. 64, 1974 pp. 775-816.
- <sup>23</sup>Ahmed, K.A. and Forliti, D.J. "Flame Holding and Combustion Characteristics of a Geometrical Flame Holder", 2008 ASME Summer Heat Transfer Conference, ASME, Jacksonville, FL, 2008.
- <sup>24</sup>Soteriou, M.C. and Ghoniem, A.F., "On the Effects of the Inlet Boundary Condition on the Mixing and Burning in Reacting Shear Flows," *Combustion and Flame*, Vol. 112, No. 3, 1998, pp. 404-417.
- <sup>25</sup>Soteriou, M.C. and Ghoniem, A.F., "The Vorticity Dynamics of an Exothermic, Spatially-Developing, Forced, Reacting Shear Layer," *Proceedings of the Combustion Institute*, Vol. 25, 1994, pp. 1265-1265.
- <sup>26</sup>Sinibaldi, J.O., Mueller, C.J., Tulkki, A.E., and Driscoll, J.F., "Suppression of Flame Wrinkling by Buoyancy: The Baroclinic Stabilization Mechanism," *AIAA Journal*, Vol. 36, No. 8, 1998, pp. 1432-1438.
- <sup>27</sup>Kiesewetter, F., Konle, M., and Sattelmayer, T., "Analysis of Combustion Induced Vortex Breakdown Driven Flame Flashback in a Premix Burner with Cylindrical Mixing Zone," *Journal of Engineering for Gas Turbines and Power*, Vol. 129, 2007, pp. 929.
- <sup>28</sup>Pan, K.L., Qian, J., Law, C.K., and Shyy, W., "The Role of Hydrodynamic Instability in Flame-Vortex Interaction," *Proceedings of the Combustion Institute*, Vol. 29, No. 2, 2002, pp. 1695-1704.
- <sup>29</sup>Renard, P.H., Thévenin, D., Rolon, J.C., and Candel, S., "Dynamics of Flame/Vortex Interactions," *Progress in Energy and Combustion Science*, Vol. 26, No. 3, 2000, pp. 225-282.
- <sup>30</sup>Chan, C.K., Wang, H.Y., and Tang, H.Y., "Effect of Intense Turbulence on Turbulent Premixed V-Flame," *International Journal of Engineering Science*, Vol. 41, No. 8, 2003, pp. 903-916.
- <sup>31</sup>Soteriou, M.C. and Ghoniem, A.F., "Effects of the Free-Stream Density Ratio on Free and Forced Spatially Developing Shear Layers," *Physics of Fluids*, Vol. 7, 1995, pp. 2036.
- <sup>32</sup>Soika, A., Dinkelacker, F., and Leipertz, A., "Pressure Influence on the Flame Front Curvature of Turbulent Premixed Flames: Comparison between Experiment and Theory," *Combustion and Flame*, Vol. 132, No. 3, 2003, pp. 451-462.
- <sup>33</sup>Mueller, C.J., Driscoll, J.F., Reuss, D.L., Drake, M.C., and Rosalik, M.E., "Vorticity Generation and Attenuation as Vortices Convect through a Premixed Flame," *Combustion and Flame*, Vol. 112, No. 3, 1998, pp. 342-358.
- <sup>34</sup>Mueller, C.J., Driscoll, J.F., Sutkus, D.J., Roberts, W.L., Drake, M.C., Smooke, M.D., Trouve, A., and Swaminathan, N., "Effect of Unsteady Stretch Rate on Oh Chemistry During a Flame-Vortex Interaction: To Assess Flamelet Models," *Combustion and flame*, Vol. 100, No. 1-2, 1995, pp. 323-331.
- <sup>35</sup>Ghoniem, A.F., Annaswamy, A., Wee, D., Yi, T., and Park, S., "Shear Flow-Driven Combustion Instability: Evidence, Simulation, and Modeling," *Proceedings of the Combustion Institute*, Vol. 29, No. 1, 2002, pp. 53-60.
- <sup>36</sup>Hammond, D.A. and Redekopp, L.G., "Local and Global Instability Properties of Separation Bubbles," *European Journal of Mechanics B-Fluids*, Vol. 17, No. 2, 1998, pp. 145-164.
- <sup>37</sup>Huerre, P. and Monkewitz, P.A., "Absolute and Convective Instabilities in Free Shear Layers," *Journal of Fluid Mechanics*, Vol. 159, 1985, pp. 151-168.
- <sup>38</sup>Jendoubi, S. and Strykowski, P.J., "Absolute and Convective Instability of Axisymmetric Jets with External Flow," *Physics of Fluids*, Vol. 6, No. 9, 1994, pp. 3000-3009.